

## Electronic Supplementary Information

### Nanostructural Dependence of Hydrogen Production in Silicon Photocathode

*Uk Sim, Hui-Yun Jeong, Tae-Youl Yang, and Ki Tae Nam\**

List of supporting figures and table.

**Figure S1.** SEM images of cross-sectional views of p-type (100) Si wafers etched in 5M HF and 0.02 M AgNO<sub>3</sub> solution at different etching times. Each of the etching time is (a) 10 min, (b) 30 min, (c) 60 min, (d) 120 min, (e) 140 min, (f) 160 min, (g) 180 min, (h) 200 min, (i) 300 min, and (j) 480 min.

**Figure S2.** SEM images of top views of p-type (100) Si wafers etched in 5M HF and 0.02 M AgNO<sub>3</sub> solution at different etching times. Each of the etching time is (a) 30 min, (b) 120 min, (c) 300 min, (d) 480 min. (a)-(b) porous, and (c)-(d) nanowire structure are observed.

**Figure S3.** Photoelectrochemical performance of planar Si structure as a function of light intensity. Black: 100mW cm<sup>-2</sup>, red: 130 mW cm<sup>-2</sup>, blue:160 mW cm<sup>-2</sup>, dark green:190 mW cm<sup>-2</sup>, pink: 216 mW cm<sup>-2</sup>.

**Figure S4.** Optical reflectance of planar Si surface and Si nanowire surface. (a) Diffuse reflectance mode and (b) specular reflectance mode. Black line indicates planar Si and red line indicates Si nanowire.

**Figure S5.** Plot of  $(\alpha hv)^{1/2}$  vs.  $hv$  for planar Si and Si nanowire from various absorption spectrum models<sup>1-3</sup>. Each model is based on the following assumption; (a)  $\alpha = A = 1 - R - T$ , (b)  $\alpha = -1/d \times \ln(R+T)$ , (c)  $\alpha = 2 - \log(\%T)$ , and (d)  $\alpha = -1/d \times \ln(T/(1-R)^2)$ .  $\alpha$  is the absorption coefficient,  $hv$  is the photon energy,  $\nu$  is the frequency,  $h$  is the Planck's constant,  $A$  is the absorbance,  $R$  is the reflectance,  $T$  is the transmittance, and  $d$  is the optical path length.

**Figure S6.** The photoelectrochemical performance of p-type Si based photoelectrodes without Pt and with Pt catalyst on Si surface as a function of etching time. (a) Limiting current density, (b) current density at 0 V vs. RHE, (c) onset potential, and (d) solar-to-hydrogen (STH) conversion efficiency.

**Figure S7.** Photographs taken during CV measurement for planar Si (left) and nanostructured Si (right). Inset images are the enlarged photographs of illumination area.

**Table S1.** Summary of the photoelectrochemical performance of p-type Si based photoelectrode. Performance of reported Si electrode for water splitting was compared with our study. The successful performances of our data are highlighted in gray. N/A indicates that there was a difficulty in estimating the values due to the lack of availability of full data set in the report.

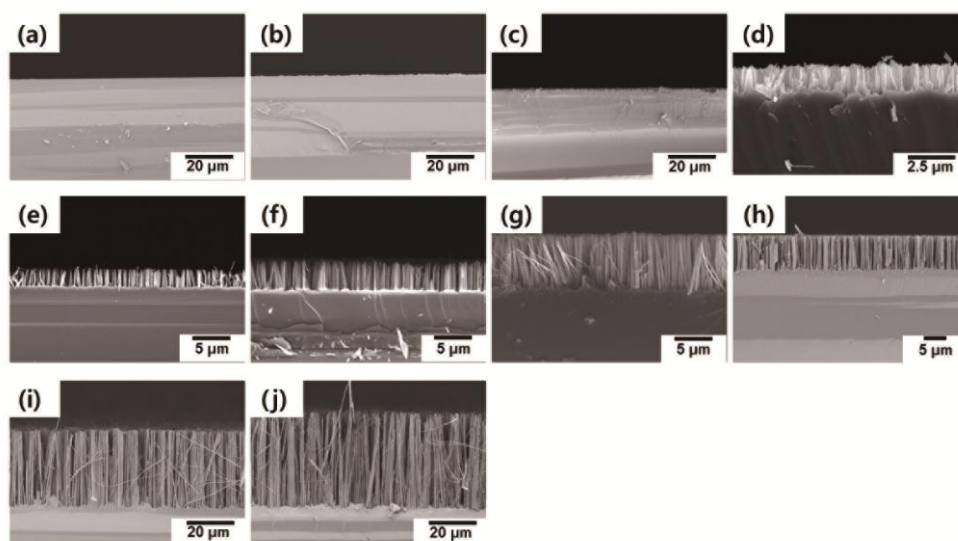


**Figure S1.** SEM images of cross-sectional views of p-type (100) Si wafers etched in 5M HF and 0.02 M AgNO<sub>3</sub> solution at different etching times. Each of the etching time is (a) 10 min, (b) 30 min, (c) 60 min, (d) 120 min, (e) 140 min, (f) 160 min, (g) 180 min, (h) 200 min, (i) 300 min, and (j) 480 min.

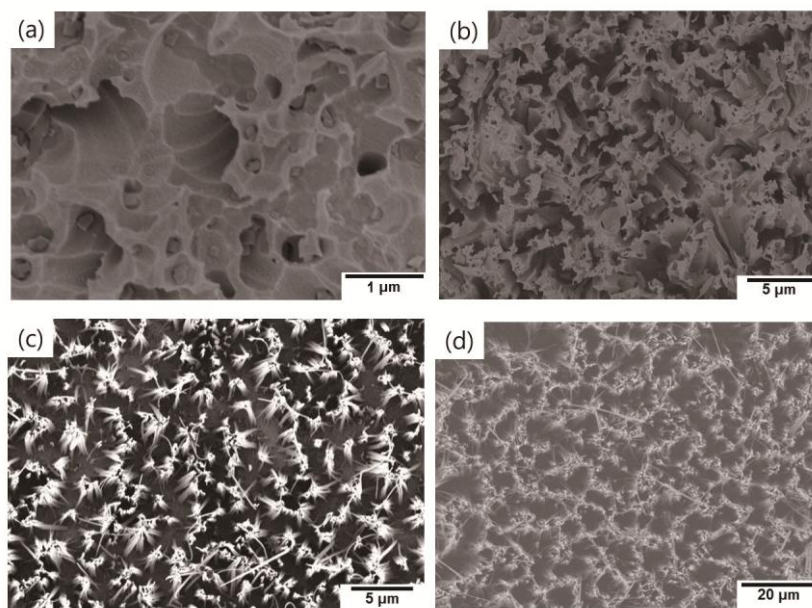


**Figure S2.** SEM images of top views of p-type (100) Si wafers etched in 5M HF and 0.02 M AgNO<sub>3</sub> solution at different etching times. Each of the etching time is (a) 30 min, (b) 120 min, (c) 300 min, (d) 480 min. (a)-(b) porous, and (c)-(d) nanowire structure are observed.

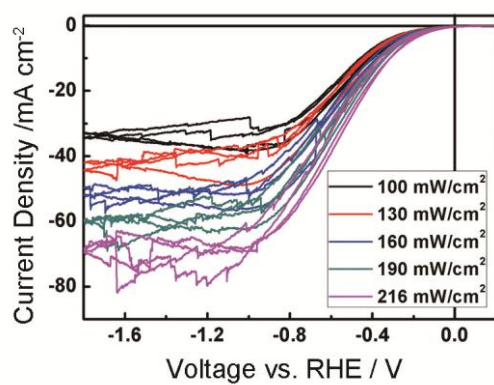


**Figure S3.** Photoelectrochemical performance of planar Si structure as a function of light intensity. Black: 100mW cm<sup>-2</sup>, red: 130 mW cm<sup>-2</sup>, blue:160 mW cm<sup>-2</sup>, dark green:190 mW cm<sup>-2</sup>, pink: 216 mW cm<sup>-2</sup>.

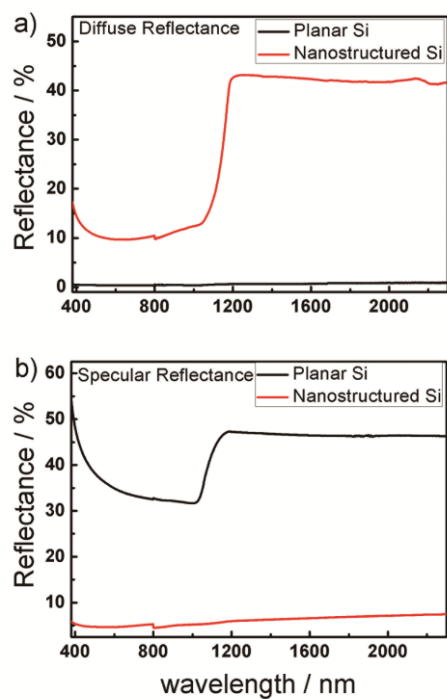


**Figure S4.** Optical reflectance of planar Si surface and Si nanowire surface. (a) Diffuse reflectance mode and (b) specular reflectance mode. Black line indicates planar Si and red line indicates Si nanowire.

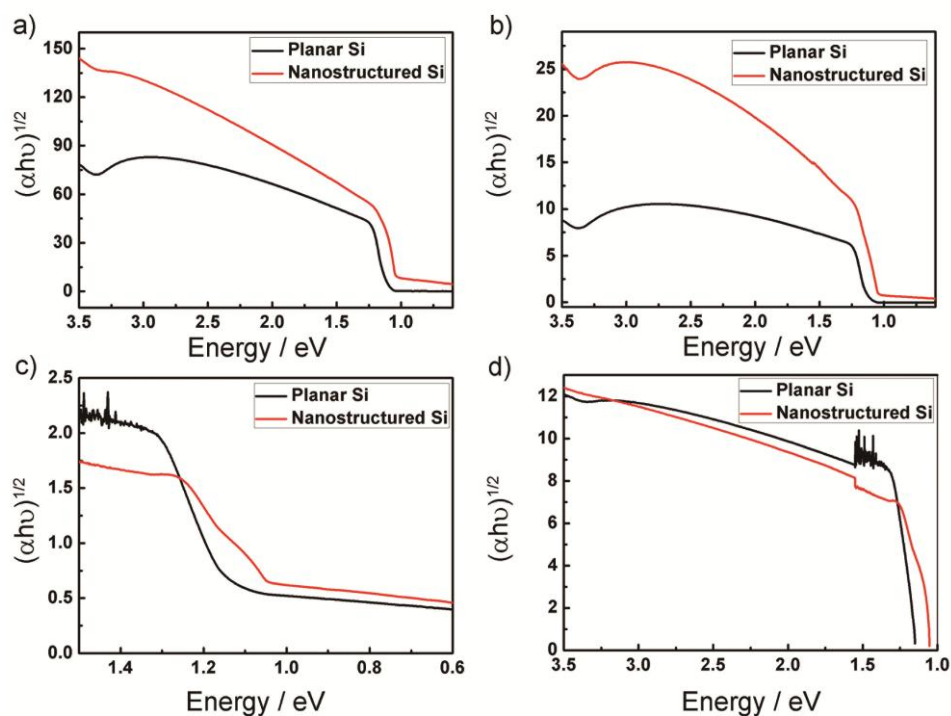


**Figure S5.** Plot of  $(\alpha h\nu)^{1/2}$  vs.  $h\nu$  for planar Si and Si nanowire from various absorption spectrum models<sup>1-3</sup>. Each model is based on the following assumption; (a)  $\alpha = A = 1 - R - T$ , (b)  $\alpha = -1/d \times \ln(R+T)$ , (c)  $\alpha = 2 - \log(\%T)$ , and (d)  $\alpha = -1/d \times \ln(T/(1-R)^2)$ .  $\alpha$  is the absorption coefficient,  $h\nu$  is the photon energy,  $\nu$  is the frequency,  $h$  is the Planck's constant,  $A$  is the absorbance,  $R$  is the reflectance,  $T$  is the transmittance, and  $d$  is the optical path length.

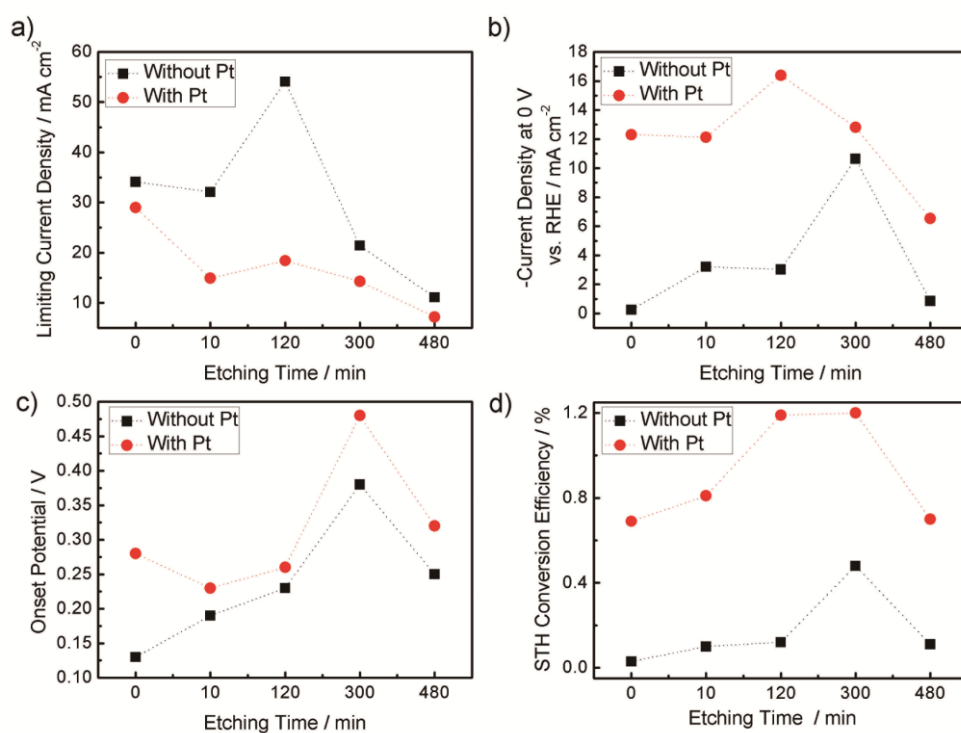


**Figure S6.** The photoelectrochemical performance of p-type Si based photoelectrodes without Pt and with Pt catalyst on Si surface as a function of etching time. (a) Limiting current density, (b) current density at 0 V vs. RHE, (c) onset potential, and (d) solar-to-hydrogen (STH) conversion efficiency.

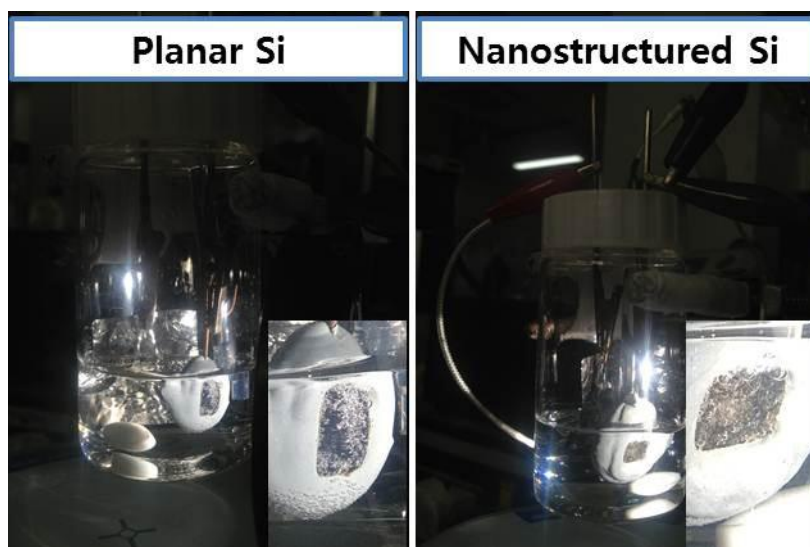


**Figure S7.** Photographs taken during CV measurement for planar Si (left) and nanostructured Si (right). Inset images are the enlarged photographs of illumination area.

**Table S1.** Summary of the photoelectrochemical performance of p-type Si based photoelectrode. Performance of reported Si electrode for water splitting was compared with our study. The successful performances of our data are highlighted in gray. N/A indicates that there was a difficulty in estimating the values due to the lack of availability of full data set in the report.

Structure	Limiting current density [mA cm <sup>-2</sup> ]	Current density at 0 V vs. RHE [mA cm <sup>-2</sup> ]	Onset potential [V]	Solar-to-Hydrogen Conversion Efficiency [%]	Ref.
Planar Si	-34.1	-0.25	0.13	0.03	
Planar Si with Pt	-29.0	-12.3	0.28	0.69	
Porous Si <sup>a)</sup> (10 min etching)	-32.1	-3.21	0.19	0.10	
Porous Si with Pt <sup>a)</sup> (10 min etching)	-14.9	-12.13	0.23	0.81	
Porous Si <sup>a)</sup> (20 min etching)	-43.4	-3.07	0.31	0.12	
Porous Si <sup>a)</sup> (30 min etching)	-45.8	-2.29	0.28	0.08	
Porous & 1.5 μm Nanowire <sup>a)</sup> (120 min etching)	-54.1	-3.02	0.23	0.12	
Porous & 1.5 μm Nanowire with Pt <sup>a)</sup> (120 min etching)	-18.4	-16.4	0.26	1.19	This study
7.1 μm Si Nanowire <sup>a)</sup> (180 min etching)	-29.9	-8.08	0.32	0.31	
7.5 μm Si Nanowire <sup>a)</sup> (200 min etching)	-27.9	-4.51	0.31	0.18	
29.3 μm Si Nanowire <sup>a)</sup> (300 min etching)	-21.4	-10.65	0.38	0.48	
29.3 μm Si Nanowire <sup>a)</sup> with Pt (300 min etching)	-14.3	-12.81	0.48	1.20	
38.0 μm Si Nanowire <sup>a)</sup> (480 min etching)	-11.1	-0.86	0.25	0.11	
38.0 μm Si Nanowire with Pt <sup>a)</sup> (480 min etching)	-7.2	-6.54	0.32	0.70	
Planar Si	-11.8	N/A	N/A	N/A	
Planar Si with Mo <sub>3</sub> S <sub>4</sub> catalyst	-10.5	-9	N/A	N/A	4
Si Microwire <sup>b)</sup>	-16.5	-0.4	N/A	N/A	
Microwire with Mo <sub>3</sub> S <sub>4</sub> catalyst <sup>b)</sup>	-14	-10	N/A	N/A	
Planar Si	-30	N/A	N/A	N/A	5
Nanoporous Si <sup>a)</sup>	-36	N/A	N/A	N/A	
Planar Si	N/A	~0 <sup>c)</sup>	~0.1 <sup>c)</sup>	N/A	
Planar with Pt	-29	-27 <sup>c)</sup>	~0 <sup>c)</sup>	N/A	6
Si Nanowire <sup>a)</sup>	-27	~0 <sup>c)</sup>	0.33	N/A	
Nanowire with Pt <sup>a)</sup>	-18	-17 <sup>c)</sup>	0.42	N/A	
Planar Si	N/A	0.82	0.255	0.03	
Planar with Pt	N/A	21.8	0.230	1.1	7
Si Microwire <sup>b)</sup>	N/A	0.005	0.034	0	
Microwire with Pt <sup>b)</sup>	N/A	11.7	0.265	1.0	

Planar Si	N/A	0.28	0.232	~0.02 <sup>c)</sup>	8
Si Wire <sup>b)</sup>	N/A	1.43	0.389	~0.14 <sup>c)</sup>	
Planar Si with Pt <sup>b)</sup>	N/A	23	0.30	2.1	9
Wire with Pt <sup>b)</sup>	N/A	7.3	0.16	0.21	

<sup>a)</sup>Wire fabricated by the metal-catalyzed electroless etching method; <sup>b)</sup>Wire grown by the vapor-liquid-solid method; <sup>c)</sup>Values were measured and extrapolated by our group referring to the figures and data from other papers.

## References

- [1] C. Wu, C. H. Crouch, L. Zhao, J. E. Carey, R. Younkin, J. A. Levinson, E. Mazur, R. M. Farrell, P. Gothoskar and A. Karger *Appl. Phys. Lett.*, 2001, **78** 1850-1851.
- [2] J. D. J. Ingle and S. R. Crouch *Spectrochemical Analysis*, Prentice Hall, NJ, USA, 1988.
- [3] S. Koynov, M. S. Brandt and M. Stutzmann *J. Appl. Phys.*, 2011, **110**, 043537.
- [4] Y. D. Hou, B. L. Abrams, P. C. K. Vesborg, M. E. Bjorketun, K. Herbst, L. Bech, A. M. Setti, C. D. Damsgaard, T. Pedersen, O. Hansen, K. Rossmesl, S. Dahl, J. K. Norskov and I. Chorkendorff, *Nat. Mater.* 2011, **10**, 434-441.
- [5] J. Oh, T. G. Deutsch, H. C. Yuan and H. M. Branz, *Energy Environ. Sci.*, 2011, **4**, 1690-1694.
- [6] I. Oh, J. Kye and S. Hwang, *Nano Lett.*, 2012, **12**, 298-302.
- [7] J. R. McKone, E. L. Warren, M. J. Bierman, S. W. Boettcher, B. S. Brunschwig, N. S. Lewis and H. B. Gray, *Energy Environ. Sci.*, 2011, **4**, 3573-3583.
- [8] J. R. Maiolo, B. M. Kayes, M. A. Filler, M. C. Putnam, M. D. Kelzenberg, H. A. Atwater and N. S. Lewis, *J. Am. Chem. Soc.*, 2007, **129**, 12346-12352.
- [9] S. W. Boettcher, E. L. Warren, M. C. Putnam, E. A. Santori, D. Turner-Evans, M. D. Kelzenberg, M. G. Walter, J. R. McKone, B. S. Brunschwig, H. A. Atwater and N. S. Lewis, *J. Am. Chem. Soc.*, 2011, **133**, 1216-1219